Research Paper

PAIN®

OPEN VIDEO

Changes to the activity and sensitivity of nerves innervating subchondral bone contribute to pain in late-stage osteoarthritis

Michael Morgan, Jenny Thai, Vida Nazemian, Richard Song, Jason J. Ivanusic*

Abstract

Although it is clear that osteoarthritis (OA) pain involves activation and/or sensitization of nociceptors that innervate knee joint articular tissues, much less is known about the role of the innervation of surrounding bone. In this study, we used monoiodoacetate (MIA)-induced OA in male rats to test the idea that pain in OA is driven by differential contributions from nerves that innervate knee joint articular tissues vs the surrounding bone. The time-course of pain behavior was assayed using the advanced dynamic weight-bearing device, and histopathology was examined using haematoxylin and eosin histology. Extracellular electrophysiological recordings of knee joint and bone afferent neurons were made early (day 3) and late (day 28) in the pathogenesis of MIA-induced OA. We observed significant changes in the function of knee joint afferent neurons, but not bone afferent neurons, at day 3 when there was histological evidence of inflammation in the joint capsule, but no damage to the articular cartilage or subchondral bone. Changes in the function of bone afferent neurons were only observed at day 28, when there was histological evidence of damage to the articular cartilage and subchondral bone. Our findings suggest that pain early in MIA-induced OA involves activation and sensitization of nerves that innervate the joint capsule but not the underlying subchondral bone, and that pain in late MIA-induced OA involves the additional recruitment of nerves that innervate the subchondral bone. Thus, nerves that innervate bone should be considered important targets for development of mechanism-based therapies to treat pain in late OA.

Keywords: osteoarthritis, osteoarthritis pain, bone afferent neurons, bone nociceptors

1. Introduction

Osteoarthritis (OA) is a chronic inflammatory condition of the joints leading to swelling, stiffness, and pain. It is characterized by focal loss of articular cartilage in synovial joints and is associated with varying degrees of synovitis and subchondral bone damage.[11] Although the focus on finding treatments for OA has been on stopping or slowing disease progression, significant improvements to quality of life and economic burden can be made by treating the underlying pain and thereby prolonging the time to joint replacement surgery. The joint capsule, synovium, and subchondral bone are all innervated by nerve endings that are activated and sensitized by noxious stimuli[24,27,28,31,33,39,47–49,54,74] and therefore constitute targets for mechanism-based therapies to treat OA pain.

There has been significant focus on the innervation of the articular tissues because of the ease of experimental access in animal models. Both the synovium and joint capsule are innervated by nociceptors that respond to noxious mechanical stimulation and known algesic substances, and that can be sensitized by inflammatory mediators in OA.[4,6,8,23,31,42,43,54,59,65] In studies of humans with OA, synovitis provokes pain via mediators of inflammation and there are reports of associations between knee pain and the degree of OA synovitis.[26,75] However, whereas radiographic evidence of joint damage predisposes to pain, the severity of the damage to the joint bears little relation to the severity of the pain experienced.[9,17,34,38] This suggests that activation of articular nociceptors may not be the critical factor for severe pain experienced by patients with OA.

In recent years, there has been a growing awareness of the involvement of subchondral bone in the pathogenesis of OA pain.[20,32,72] When articular cartilage breaks down with disease progression, several changes in the subchondral bone become obvious, including osteochondral channels, microdamage, bone marrow edema, and bone cysts.[7,18] This is the most debilitating stage of the disease for which pain management is most problematic. Of particular relevance, severe pain in patients with OA is clearly correlated with radiological evidence of subchondral bone lesions or inflammation, and the severity of pain is correlated with the size of lesions.[2,16,36,75] There is also speculation from experiments conducted during joint replacement surgery that in advanced OA, severe pain may be caused by raised intraosseous pressure in the bones around joints.[10,70] Thus, it seems that

Sponsorships or competing interests that may be relevant to content are disclosed at the end of this article.

Department of Anatomy and Physiology, University of Melbourne, Victoria, Australia

**Corresponding author. Address: Department of Anatomy and Physiology, University of Melbourne, Melbourne, VIC 3010, Australia. E-mail address: j.ivanusic@unimelb.edu.au (J. Ivanusic).*

Supplemental digital content is available for this article. Direct URL citations appear in the printed text and are provided in the HTML and PDF versions of this article on the journal's Web site (www.painjournalonline.com).

PAIN 163 (2022) 390–402

http://dx.doi.org/10.1097/j.pain.0000000000002355

subchondral bone is more important in the pathogenesis of OA pain than originally thought, particularly at late-stage OA when there is cartilage breakdown, and that changes to the function of nerves that innervate the surrounding bone may drive pain during this late stage of disease.

In this study, we have used electrophysiology to record directly from nerves that innervate the knee joint and surrounding bones in a rat model of monoiodoacetate (MIA)-induced OA, to determine how OA affects their function.

2. Methods

2.1. Animals

Male Sprague-Dawley rats weighing between 200 and 250 g were used in this study. Animals were housed in pairs in a 12-hour light/dark cycle and were provided with food and water ad libitum. All experiments conformed to the Australian National Health and Medical Research Council code of practice for the use of animals in research and were approved by the University of Melbourne Animal Experimentation Ethics Committee.

2.2. Induction of osteoarthritis

Osteoarthritis was induced by injection of MIA (Sigma-Aldrich, St Louis, MO) into the left knee joint of animals. This is an established model that is characterized by an acute inflammatory response in the first week post-MIA injection, and significant cartilage breakdown and damage to subchondral bone later in disease progression.[19] It results in rapid and reproducible changes in weight-bearing (within a day post-MIA injection) that are related to acute inflammation of the knee joint. Pain behavior persists beyond 28 days at which point it is also associated with damage of subchondral bone.[19,46] Although the time-course of pain behavior and histopathology in MIA-induced OA is not entirely consistent with what is observed in humans with OA, the model provides the opportunity to explore how inflammation of the joint, and/or damage to subchondral bone, can impact on the function of nerves innervating the knee joint and surrounding bone. Animals were anesthetized with isoflurane (4% induction; 2.5% maintenance). A topical local anesthetic (2% lignocaine) was applied to the skin at the injection site and animals were given an intra-articular injection of MIA (4.5 mg/50 μL, in sterile saline). We chose a high dose (4.5 mg) of MIA to ensure we were able to observe significant changes in bone in a reasonable experimental timeframe. Control animals received an intra-articular injection of sterile saline (50 μL). In both cases, the solution was injected slowly and the joint gently massaged after the needle was removed.

2.3. Dynamic weight-bearing to assay pain behavior

Weight-bearing was evaluated using the advanced dynamic weight-bearing device (Bioseb, Boulogne, France) (**Fig. 1A**). This apparatus consists of a clear Plexiglas chamber (22 × 22 × 30 cm), and a sensory pad composed of 1936 pressure transducers, which is synchronized to a video camera mounted to the top of the enclosure. This allows for simultaneous and automated exploration of weight-bearing on each paw during movement of the animals around the chamber and requires minimal animal handling. Animals were habituated to the device 1 day before surgery. Behavioral testing was performed to generate a baseline metric on the day of OA induction (day 0), and then at days 1, 2, 3, 4, 5, 7, 9, 11, 15, 18, 20, 23, and 28 after surgery, to establish the time-course of pain behavior in MIA-induced OA. Testing was performed by the same experimenter and at the same time each day, and analysis was performed blinded to the experimental condition. The animals were allowed to move freely within the chamber for 4 minutes at each testing time-point. The data were analyzed, by a blinded investigator, using the advanced dynamic weight-bearing device software (module version 1.4.3.98; Bioseb). This involved assigning pressure zones to the corresponding paws (front left, front right, rear left, and rear right) for each time segment of the data. A zone was considered valid when one pressure transducer recorded a weight of ≥4 g and at least 2 adjacent pressure transducers recorded a weight of ≥2 g. A time segment was considered valid if the activated zones were stable for ≥0.5 seconds. Animals were excluded if there was less than 60 seconds of total validated time available, if there was excessive grooming behavior during the recording period, or if animals were exhibiting freezing behavior. Weight borne on the hind limb injected with MIA or saline was expressed as a percentage of the total weight borne on both hind limbs.

2.4. Histological assessment of joint and subchondral bone pathology

Histological changes in the knee joint and surrounding bones were assessed using haematoxylin and eosin at days 3 or 28 after injection of MIA or saline. Haematoxylin and eosin was used because it allows for easy identification of changes to both the cartilage and surrounding bone, particularly in late MIA-induced OA, and because it is easier to apply compared with other stains. Animals were anaesthetized with an overdose of ketamine/xylazine (ketamine 130 mg/kg, xylazine 10 mg/kg; i.p.) and were perfused via the ascending aorta with 500 mL heparinized phosphate buffered saline (PBS) followed by 500 mL of 4% paraformaldehyde in PBS. The hind limb was removed and the knee joint was dissected away from surrounding soft tissues, paying careful attention to conserving the joint capsule and surrounding subchondral bone. Dissected joints were postfixed in 4% paraformaldehyde for 72 hours, washed in PBS, and decalcified in 5% formic acid in water for 7 days. The formic acid solution was changed every second day. The joints were washed in running tap water, embedded in paraffin, and serially sectioned in the coronal plane, at 100 μm intervals, into 4-μm-thick sections. The sections were deparaffinized in xylene, rehydrated in 100% and 70% ethanol followed by water, stained with haematoxylin and eosin, dehydrated in 100% ethanol, and cleared in xylene before being mounted onto glass slides with CV mounting medium (Leica, Illinois). Sections were scored and imaged with 2.5x objective and 10x objective using a Zeiss Axioskop fluorescence microscope (Zeiss, Oberkochen, Germany) fitted with an AxioCam MRm camera.

Histological changes to the joint and surrounding bone was scored by a blinded investigator using a modified Osteoarthritis Research Society International scale.[21] **Table 1** outlines the specific criteria used to score synovitis (thickening of the synovial lining and infiltration of inflammatory cells), proteoglycan loss, chondrocyte hypertrophy and clustering, cartilage breakdown, subchondral bone changes, and the formation of osteophytes. Scores ranged from zero (normal structure without any pathology) to 3 (severe pathology) (**Table 1**).

2.5. Electrophysiological recordings

We used in vivo electrophysiology to determine how the function of knee joint and/or bone afferent neurons is affected by MIA-induced OA (**Fig. 2**). Recordings were made at either day 3 (when evidence of histopathology is confined principally to the joint

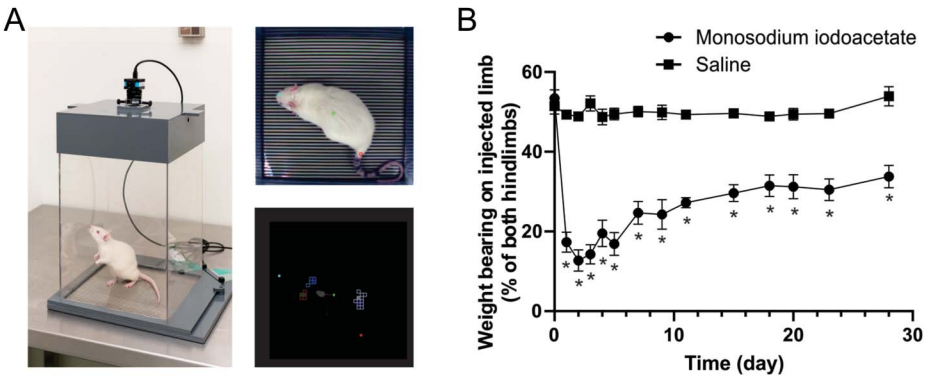

Figure 1. Time-course of MIA-induced pain behavior. (A) Weight-bearing was assessed using the advanced dynamic weight-bearing assay that measures distribution of weight-bearing across each limb. (B) There was a significant reduction in weight-bearing on the injected hind limb, relative to the uninjected hind limb, in MIA (n = 9) relative to saline (n = 10) injected animals, at all time-points tested (Bonferroni post hoc test $^*P < 0.05$). Peak reduction in weight-bearing for MIA-injected animals occurred at days 2 and 3, and weight-bearing was still markedly reduced at day 28. Data represent mean ± SEM. MIA, monoiodoacetate.

capsule) or day 28 (when significant involvement of subchondral bone is evident).

Rats were anesthetized with urethane (50% wt/vol, 1.5 g/kg; i.p.). Rectal temperature was maintained within the physiological range (36-37°C) with a servo-controlled heating pad. Dissections were made to expose the medial articular nerve that innervates the rat knee joint capsule,[29] or a small nerve that innervates the subchondral bone of the rat tibia.[47–49] The medial articular nerve was exposed by making a skin incision over the medial aspect of the knee and thigh, and cutting it away from its parent saphenous nerve. The nerve to the rat tibia was exposed by making a skin incision along the medial aspect of the tibia, and removing the medial head of the gastrocnemius muscle, to identify the nerve entering bone at the posteromedial aspect of the tibia. Each nerve was carefully teased away from its associated blood vessels and membranes and placed on a platinum hook electrode for extracellular recording. A second, indifferent electrode was implanted into nearby muscle. The nerves were protected from desiccation by using skin and/or muscle flaps to create a paraffin-filled pool that was maintained at room temperature. The sciatic and femoral nerves were transected high in the limb to prevent reflex activation of muscle or sympathetic efferent fibers in the nerves that we recorded from. Whole-nerve electrical activity was amplified (×1000) and filtered (high pass 100 Hz, low pass 3 kHz) (DP-311 differential amplifier, Warner Instruments), sampled at 20 kHz (PowerLab; ADInstruments, Bella Vista, Australia), and stored to PC using LabChart recording software (ADInstruments).

Receptive fields of knee joint afferent neurons were identified by mechanical stimulation, delivered by applying a series of calibrated von Frey filaments (up to 4 g) to their peripheral

Table 1

Scoring criteria for histopathology.

Score	0—normal	1—mild	2—moderate	3—severe
Synovitis	1 layer of synovial lining cells; no inflammatory cell infiltration	2-3 layers of synovial lining cells, no or mild inflammatory cell infiltration	4-5 layers of synovial lining cells, moderate inflammatory cell infiltration	>5 layers of synovial lining cells, significant inflammatory cell infiltration
Proteoglycan loss	No proteoglycan loss	Proteoglycan loss in the superficial part of the cartilage	Proteoglycan loss in the superficial and middle parts of the cartilage	Proteoglycan loss through the full thickness of the cartilage
Chondrocyte hypertrophy and clustering	No hypertrophy or decrease in number of chondrocytes, no loss of columns, <5 cells/cluster	Hypertrophy and focal decrease in number of chondrocytes at the surface of the cartilage, mild loss of columns, <5 cells/cluster	Hypertrophy and multifocal decreases in the number of chondrocytes, moderate loss of columns, 5-7 cells/cluster	Hypertrophy and extensive decrease in number of chondrocytes, extensive loss of columns, >7 cells/cluster
Cartilage degradation	No degradation of cartilage	Fissures extending into the superficial cartilage: <10% from the cartilage surface	Fissures extending into the middle of the cartilage	Fissures extending into the deepest part of the cartilage, full thickness degradation of cartilage to the tidemark, collapse of articular cartilage into the epiphysis
Subchondral bone changes	Normal	Focal fragmentation of calcified cartilage at the tidemark	Marked fragmentation of calcified cartilage at the tidemark, mesenchymal changes involving up to 1/2 of the subchondral bone under the fragmentation	Significant fragmentation of the calcified cartilage at the tidemark, mesenchymal changes involving over 1/2 of subchondral bone under the fragmentation, may include bone cyst
Osteophyte formation	Minimal proliferative changes <200 μm diameter	Osteophyte: 200-299 μm in diameter	Osteophyte: 300-399 μm in diameter	Osteophyte >400 μm in diameter

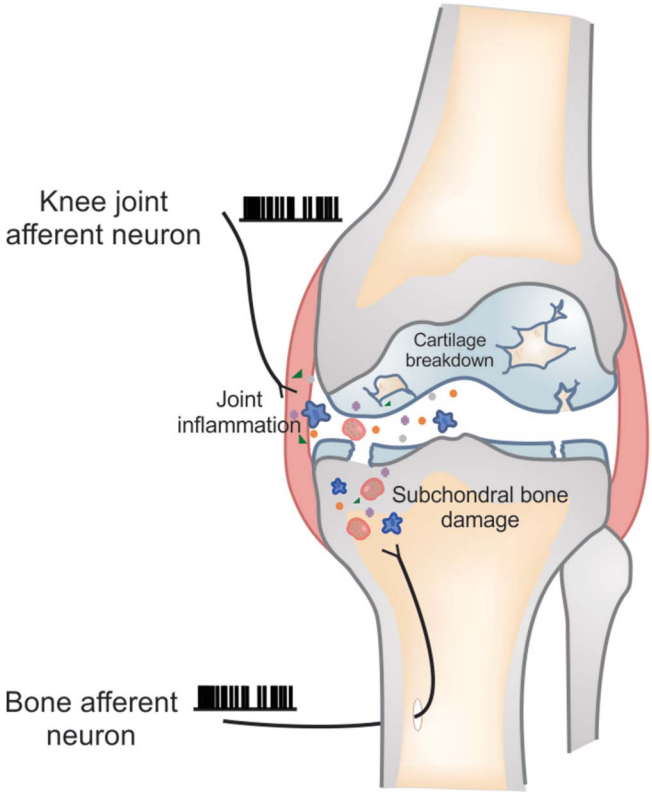

Figure 2. Schematic of the knee joint showing key features of monoiodoacetate-induced osteoarthritis and approaches to recording from nerves that innervate the joint capsule vs subchondral bone.

endings in the medial aspect of the joint capsule. Each filament was applied perpendicular to the surface of the joint capsule and was maintained for at least 4 seconds. The receptive fields of knee joint afferent neurons identified in this way are relatively discrete, so spikes arising from single, mechanically sensitive knee joint afferent neurons were easily discriminated from the whole-nerve recordings by their similar amplitude and duration. The threshold for mechanical activation of each of the discriminable knee joint afferent neurons was defined at the lowest force filament that produced action potential discharge. Discharge frequency was calculated from the number of action potentials that fired during the first 4 seconds of a suprathreshold stimulus (4 g von Frey stimulation) and was expressed as the number of action potentials/second (Hz). The location of receptive fields was mapped on a diagram, relative to clear landmarks such as blood vessels etc.

Receptive fields of bone afferent neurons buried deep in the marrow cavity were not accessible using our preparation, so mechanical stimulation was instead delivered to the endings of bone afferent neurons by raising intraosseous pressure in the marrow cavity. This was achieved by injection of heparinized (0.17 IU/mL) physiological saline (0.9% sodium chloride) through a needle that was connected to a feedback-controlled syringe pump (PHD ULTRA pump; Harvard apparatus, Holliston, MA) with polyethylene tubing. The input pressure to the bone was measured using a bridge amplified (TAM-D amplifier) signal derived from a pressure transducer (APT300 transducer), placed to measure the input pressure to the bone. The pump uses this as feedback to adjust flow through the system to control and maintain constant input pressures. We used this feature to apply a ramp-and-hold mechanical stimulus with an initial flow rate of 7 mL/min during the ramp (rising) phase, and a constant 300 mm Hg of pressure delivered for a 15-second duration during the hold phase. Nerve impulses arising from single, Aδ mechanically sensitive bone afferent neurons were discriminated from the whole-nerve recordings by their similar amplitude and duration. We were not able to isolate individual C-fiber bone afferent neurons because they did not have clearly discriminable amplitudes and/or durations. However, we report data for all spikes with amplitudes consistent with C-fiber activity in whole-nerve recordings of nerve to the rat tibia. This allows us to assess if there are changes in the discharge frequency of C-fiber bone afferent neurons at the whole-nerve level.

The threshold for mechanical activation of bone afferent neurons was calculated from the rising phase of the pressure stimulus. Discharge frequency was reported over the entire ramp-and-hold pressure stimulus and was expressed as the number of action potentials/second (Hz).

The conduction velocity of knee joint afferent neurons was determined by electrical stimulation with a bipolar silver electrode (0.5 Hz, 0.02-2 ms pulse duration, 0.05-10 V). Conduction velocity was calculated by dividing the distance between the electrical stimulation site and the recording electrode, by the time taken for an action potential elicited by the electrical stimulus to reach the recording electrode. In all cases, we were able to identify unitary spikes on electrical stimulation that matched the size and shape of spikes evoked by mechanical stimulation of the receptive field. Aδ fibers were classified as those with conduction velocities between 2.5 and 12 m/s, whereas C fibers were classified as those with conduction velocities slower than 2.5 m/s. We were unable to routinely record the conduction velocities of bone afferent neurons in each experiment because we could not electrically stimulate the receptive fields of individual units buried deep inside the marrow cavity. Instead, we classified spikes as originating from C or Aδ fibers on the basis of previously published experiments using the same recording configuration in which we demonstrated a linear relationship between conduction velocity and peak-to-peak action potential amplitude for units activated with a 300-mm Hg pressure stimulus applied to the marrow cavity (see Refs. 47 and 49). In these previous experiments, single units were discriminated in the whole-nerve recordings according to their amplitude and duration using Spike Histogram software (LabChart 8, ADInstruments). Conduction velocities were determined using 2 recording electrodes with a distance of 7 to 10 mm between electrodes. Action potentials recorded at the second electrode, which were time-locked to those recorded at the first electrode, were considered as originating in the same axon. Conduction velocities were estimated by dividing conduction time between the electrodes by the distance between electrodes. Units with Aδ conduction velocities (2.5-12.5 m/s) had action potential amplitudes between 47 to 145 μV, and units with C conduction velocities (<2.5 m/s) had small amplitude action potentials (<40 μV). Thus, in this study, we define spikes with peak-to-peak amplitudes of between 40 to 145 μV as being derived from Aδ fibers, and spikes with peak-to-peak amplitudes of less than 40 μV as derived from C fibers. Some very fast conducting units were observed but these had very large amplitude spikes (>145 μV) and had receptive fields outside of the marrow cavity (they responded to gentle probing of the periosteum or muscle adjacent to the bone). It is possible that these units represent low-threshold mechanoreceptors, in surrounding periosteum or muscle, that were mechanically activated by leakage of saline from the marrow cavity, through Volkmann canals and into surrounding tissue. They were relatively rare and were excluded from further analysis.

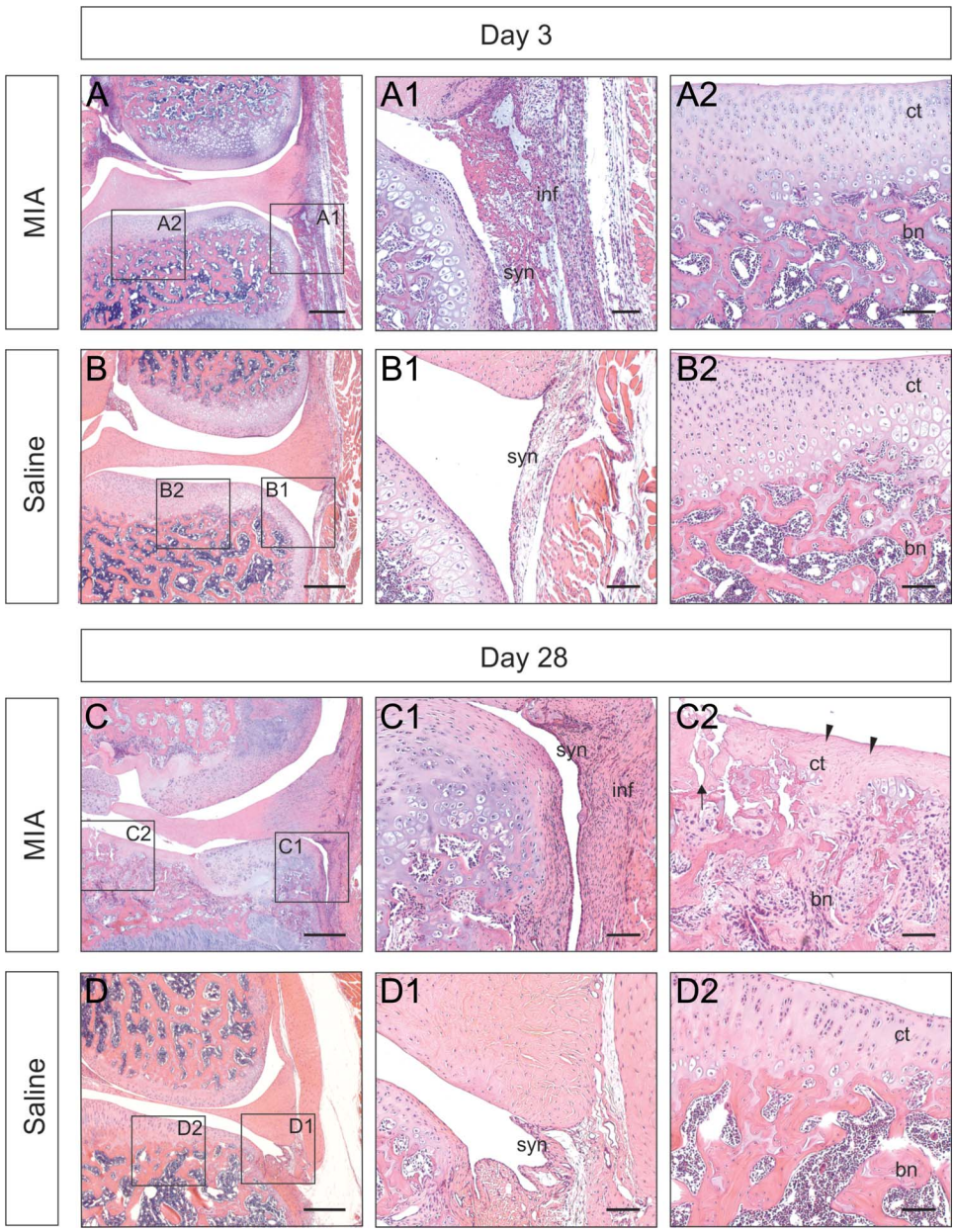

Figure 3. Monoiodoacetate-induced changes in the histology of the knee joint and surrounding bone. (A) Low-power photomicrograph of a knee joint and surrounding bone showing histological changes at 3 days post-MIA injection. Inset A1 shows a higher-power view of the synovium and the joint capsule, to highlight thickening of the synovial cell layers and inflammatory cell infiltration of the synovium and joint capsule at 3 days post-MIA injection. Inset A2 shows a higher-power view of the articular cartilage and subchondral bone, highlighting it is normal at 3 days post-MIA injection. (B) Low-power photomicrograph of a knee joint and surrounding bone showing histological changes at 3 days after saline injection. Inset B1 shows a higher-power view of the synovium and the joint capsule, to highlight normal synovium and a lack of inflammatory cell infiltration at 3 days after saline injection. Inset B2 shows a higher-power view of the articular cartilage and subchondral bone, highlighting it is normal at 3 days after saline injection. (C) Low-power photomicrograph of a knee joint and surrounding bone showing histological changes at 28 days post-MIA injection. Inset C1 shows a higher-power view of the synovium and the joint capsule, along with some articular cartilage and subchondral bone, to highlight thickening of the synovial cell layers and inflammatory cell infiltration of the synovium and joint capsule, and extensive remodeling of the subchondral bone, at 28 days post-MIA injection. Inset C2 shows a higher-power view of the articular cartilage and subchondral bone highlighting marked proteoglycan and chondrocyte loss (arrowheads), fragmentation of the articular cartilage (arrow), and extensive remodeling and inflammation of the subchondral bone. (D) Low-power photomicrograph of a knee joint and surrounding bone showing histological changes at 28 days after saline injection. Inset D1 shows a higher-power view of the synovium and the joint capsule, to highlight normal synovium and a lack of inflammatory cell infiltration at 28 days after saline injection. Inset B2 shows a higher-power view of the articular cartilage and subchondral bone highlighting it is normal at 28 days after saline injection. Scale bars in low-power photomicrographs = 500 μm. Scale bars in insets = 100 μm. syn, synovium; inf, inflammatory cell infiltration; ct, articular cartilage; bn, bone; MIA, monoiodoacetate.

To determine whether MIA-induced OA increases spontaneous activity in the medial articular nerve, or the nerve to the rat tibia, a continuous whole-nerve recording was made over a 5-minute period, 10 minutes after the nerve was applied to the electrode. All spikes with positive and/or negative peaks clearly above noise were sampled from the whole-nerve recordings, and spontaneous activity was expressed as the number of spikes per second (Hz).

To determine whether MIA-induced OA increases the mechanical sensitivity of knee joint or bone afferent neurons, comparisons of threshold for mechanical activation and discharge frequency in

Table 2

Histology scores.

Day 3—Animal #	Saline (n = 6 day 3)							MIA (n = 6 day 3)							One-sample *t* test
	#1	#2	#3	#4	#5	#6	Mean	#1	#2	#3	#4	#5	#6	Mean	
Synovitis	0	0	0	0	0	0	0	3	3	3	1	3	2	2.5	$P < 0.05$
Proteoglycan loss	0	0	0	0	0	0	0	0	0	0	0	0	0	0	ns
Chondrocyte hypertrophy and clustering	0	0	0	0	0	0	0	0	0	0	0	0	0	0	ns
Cartilage degradation	0	0	0	0	0	0	0	0	0	0	0	0	0	0	ns
Subchondral bone changes	0	0	0	0	0	0	0	0	0	0	0	0	0	0	ns
Osteophyte formation	0	0	0	0	0	0	0	0	0	0	0	0	0	0	ns
Day 28—Animal #	**Saline (n = 6 day 28)**							**MIA (n = 6 day 28)**							**One-sample *t* test**
	#1	#2	#3	#4	#5	#6	Mean	#1	#2	#3	#4	#5	#6	Mean	
Synovitis	0	0	0	0	0	0	0	1	1	1	0	1	2	1	$P < 0.05$
Proteoglycan loss	0	0	0	0	0	0	0	3	3	3	3	3	3	3	$P < 0.05$
Chondrocyte hypertrophy and clustering	0	0	0	0	0	0	0	3	3	2	3	3	3	2.8	$P < 0.05$
Cartilage degradation	0	0	0	0	0	0	0	3	3	2	1	3	3	2.5	$P < 0.05$
Subchondral bone changes	0	0	0	0	0	0	0	3	3	3	3	3	3	3	$P < 0.05$
Osteophyte formation	0	0	0	0	0	0	0	1	1	1	1	3	2	1.5	$P < 0.05$

MIA, monoiodoacetate.

response to mechanical stimulation were made between animals injected with MIA and those injected with saline (control).

All animals that were recorded from were killed by decapitation, while still anesthetized by urethane, at the end of each experiment.

2.6. Statistical analyses

Statistical analyses were performed using Prism (GraphPad Prism; GraphPad Software). Comparison of pain behavior over time was analyzed using a two-way analysis of variance (ANOVA) with repeated measures (MIA vs saline), followed by Bonferroni post hoc testing only if the ANOVA indicated a significant difference. Because the mean histological scores for the saline controls were zero and had no variance, the data for the MIA histological scores were analyzed using a one-sample *t* test (with a hypothesized mean score of zero). Comparisons of whole-nerve spontaneous activity at each time-point were made using unpaired *t* tests (MIA vs saline). Comparisons of the response of single Aδ and C knee joint afferent neurons, and Aδ bone afferent neurons, to mechanical stimulation were evaluated using a mixed-model nested *t* test (MIA vs saline). A mixed-model design was used to avoid potential errors related to pseudoreplication for electrophysiological data that included multiple cells derived from a single recording preparation. Comparisons of the response of C bone afferent neurons in whole-nerve recordings were made with unpaired *t* tests (MIA vs saline). In all cases, $P < 0.05$ was used to define statistical significance. In cases where multiple action potential units were isolated from a single recording, N = number of action potential units and n = number of animals/recordings.

Results

3.1. Changes in weight-bearing resulting from monoiodoacetate-induced osteoarthritis are established by day 1 and persist for at least 28 days

There was a rapid decrease in weight-bearing on the injected limb of MIA-injected animals, but not saline-injected animals, that was established by day 1 and persisted to at least day 28 (two-way ANOVA with repeated measures; Bonferroni multiple comparisons; **Fig. 1B**). Peak reductions in weight-bearing for MIA-injected animals occurred at days 2 and 3. Weight-bearing was relatively stable after this time and was still markedly reduced at day 28.

3.2. Histological changes are confined to the joint in early monoiodoacetate-induced osteoarthritis and extend to the bone in late monoiodoacetate-induced osteoarthritis

At day 3, MIA-injected animals had obvious histological changes associated with inflammation of the soft tissues of the joint, including thickening of the synovial lining of the joint capsule and infiltration of inflammatory cells (**Fig. 3A** and **Table 2**). However, at this time-point, there was no evidence of proteoglycan loss, chondrocyte hypertrophy and clustering, or degradation of the articular cartilage, and no evidence of fragmentation of calcified cartilage at the tidemark, mesenchymal changes, or osteophyte formation in the surrounding subchondral bone (**Fig. 3A** and **Table 2**). There were also no histological changes in saline-injected control animals (**Fig. 3B** and **Table 2**). Statistical analyses confirmed a significant increase in the score for histological findings relating to the soft tissues, but not in the score for each of the histological findings relating to articular cartilage and bone, in MIA-injected animals (one-sample *t* test; **Table 2**).

At day 28, there were still obvious histological changes associated with inflammation in the soft tissues of the joint of MIA-injected animals, albeit with a mean score that was lower than for day 3 (**Fig. 3C** and **Table 2**). However, at this same time-point, MIA-injected animals also showed clear evidence of proteoglycan loss, chondrocyte hypertrophy and clustering, degradation of the articular cartilage, fragmentation of calcified cartilage at the tidemark, and mesenchymal changes and osteophyte formation in the surrounding subchondral bone (**Fig. 3C** and **Table 2**). There were no histological changes in

saline-injected control animals at day 28 (**Fig. 3D** and **Table 2**). Statistical analyses confirmed a significant increase in the score for each of these findings in MIA-injected animals (one-sample *t* test; **Table 2**).

3.3. Electrophysiological changes are confined to knee joint afferent neurons in early monoiodoacetate-induced osteoarthritis

At day 3, the individual Aδ neurons recorded from the medial articular nerve of animals injected with MIA had reduced thresholds for mechanical activation (nested *t* test), and increased mechanically evoked discharge frequencies (nested *t* test), relative to those injected with saline (**Figs. 4A and B**). At this time-point, there was also a reduction in the threshold for mechanical activation (nested *t* test), and an increase in discharge frequency (nested *t* test), of individual C-fiber neurons recorded from the medial articular nerve of animals injected with MIA, relative to those injected with saline (**Figs. 4C and D**). In addition, spontaneous activity in whole-nerve recordings made from the medial articular nerve was markedly increased in MIA-injected animals relative to saline-injected animals (*t* test; **Fig. 4E**). Thus, knee joint afferent neurons are activated and sensitized in early MIA-induced OA and contribute to pain signaling when there is evidence of inflammation of the joint capsule.

By contrast, at day 3, there were no changes in the threshold for mechanical activation (nested *t* test), or the mechanically evoked discharge frequency (nested *t* test), of individual Aδ neurons recorded from the nerve to the rat tibia of animals injected with MIA, relative to those injected with saline (**Figs. 5A and B**). There were also no changes in the mechanically evoked discharge frequency of C-fiber neurons recorded from the nerve to the rat tibia of animals injected with MIA, relative to those injected with saline (unpaired *t* test; **Fig. 5C**). Because we were unable to isolate the activity of individual C-fiber neurons in the bone-nerve preparation, the thresholds for activation for C-fiber units could not be ascertained. In addition, there was no difference in spontaneous activity in whole-nerve recordings from the nerve to the rat tibia in MIA-injected animals, relative to saline-injected animals, at day 3 (unpaired *t* test; **Fig. 5D**). These findings indicate that bone afferent neurons have no role in pain signaling in early MIA-induced OA.

3.4. Electrophysiological changes in bone afferent neurons are evident only in late monoiodoacetate-induced osteoarthritis

At day 28, there was a reduction in the threshold for mechanical activation (nested *t* test), but no change in the mechanically evoked discharge frequency (nested *t* test), of individual Aδ neurons recorded from the medial articular nerve of animals injected with MIA, relative to those injected with saline (**Figs. 6A and B**). There was also a reduction in the threshold for mechanical activation (nested *t* test), and an increase in discharge frequency (nested *t* test), of individual C-fiber neurons recorded from the medial articular nerve of animals injected with MIA, relative to those injected with saline (**Figs. 6C and D**). Thus, knee joint afferent neurons remain sensitized even at day 28 post-MIA injection. However, at this time-point, there was no difference in spontaneous activity in whole-nerve recordings made from the medial articular nerve in MIA, relative to saline-injected animals (unpaired *t* test; **Fig. 6E**).

Importantly, at day 28, there was a reduction in the threshold for mechanical activation (nested *t* test), and an increase in the mechanically evoked discharge frequency (nested *t* test), of individual Aδ neurons recorded from the nerve to the rat tibia of animals injected with MIA, relative to those injected with saline (**Figs. 7A and B**). There was also an increase in the mechanically evoked discharge frequency of C-fiber neurons recorded from the nerve to the rat tibia of animals injected with MIA, relative to those injected with saline (unpaired *t* test; **Fig. 7C**). There was no difference in spontaneous activity in whole-nerve recordings in MIA-injected animals, relative to saline-injected animals, at day 28 (unpaired *t* test; **Fig. 7D**). These changes in activity and/or sensitivity of bone afferent neurons at day 28 were not observed at day 3 and clearly indicate that bone afferent neurons contribute to pain signaling in late MIA-induced OA, when there is evidence of histopathology in the subchondral bone.

3. Discussion

Electrophysiological recording was used to determine how nerves that innervate the knee joint and surrounding bones are affected by MIA-induced OA in the rat. We observed significant changes in the function of knee joint afferent neurons, but not bone afferent neurons, early in progression of MIA-induced OA, when there is histological evidence of inflammation in the joint capsule, but no damage to either the articular cartilage or surrounding subchondral bone. Changes in the function of bone afferent neurons occurred later in progression of MIA-induced OA, when there is histological evidence of damage to the articular cartilage and surrounding subchondral bone. Our findings suggest that pain induced by the acute inflammatory response in early MIA-induced OA involves activation and/or sensitization of nerves that innervate the joint capsule and synovium but not the underlying subchondral bone, and that pain in late MIA-induced OA involves the additional recruitment of nerves that innervate the subchondral bone.

Patients with OA often present clinically with pain during activity, stiffness, grinding, catching, swelling, and/or altered joint function.[14,15,25] Clinical examination often reveals joint line tenderness or crepitus,[14] and a lack of significant evidence of radiographical changes to the joint, scored at less than 2 on the Kellgren and Lawrence scale.[30,37] When patients experience flare-ups of night pain or morning stiffness, it is usually accompanied by joint effusion, suggesting the pain is related to inflammation.[2] Synovitis provokes pain via mediators of inflammation and there are reports of correlations between knee pain and the degree of OA synovitis.[26] Thus, inflammation of the joint capsule and synovium is likely one of the main drivers of pain in OA.

Studies using in vivo recording of joint afferent neurons in the cat and the rat report sensitization of Aδ- and/or C-fiber neurons, but not Aβ-fiber neurons, to mechanical stimulation in the presence of acute inflammation,[12,22,61] or upon application of inflammatory mediators such as IL-6, IL-17, TNF, prostaglandins, or bradykinin, among many others.[5,33,39,51,57,58,62,63] There have also been a number of studies showing that many of these features are relevant to OA and, in particular, MIA-induced OA in rats.[41,65–69] However, recordings in most of these latter studies were made at day 14 post-MIA injection, a time at which there is significant evidence of damage to articular cartilage and bone in rat MIA-induced OA. Our findings clearly show that similar changes in the function of Aδ- and C-fiber knee joint afferent neurons occur in the acute, inflammatory phase of MIA-induced OA, before there is any histological damage to the articular cartilage or surrounding bone. Thus, the early effects of MIA-induced OA on knee joint afferent neurons are likely a result of inflammation confined to the joint, and there does not seem to be

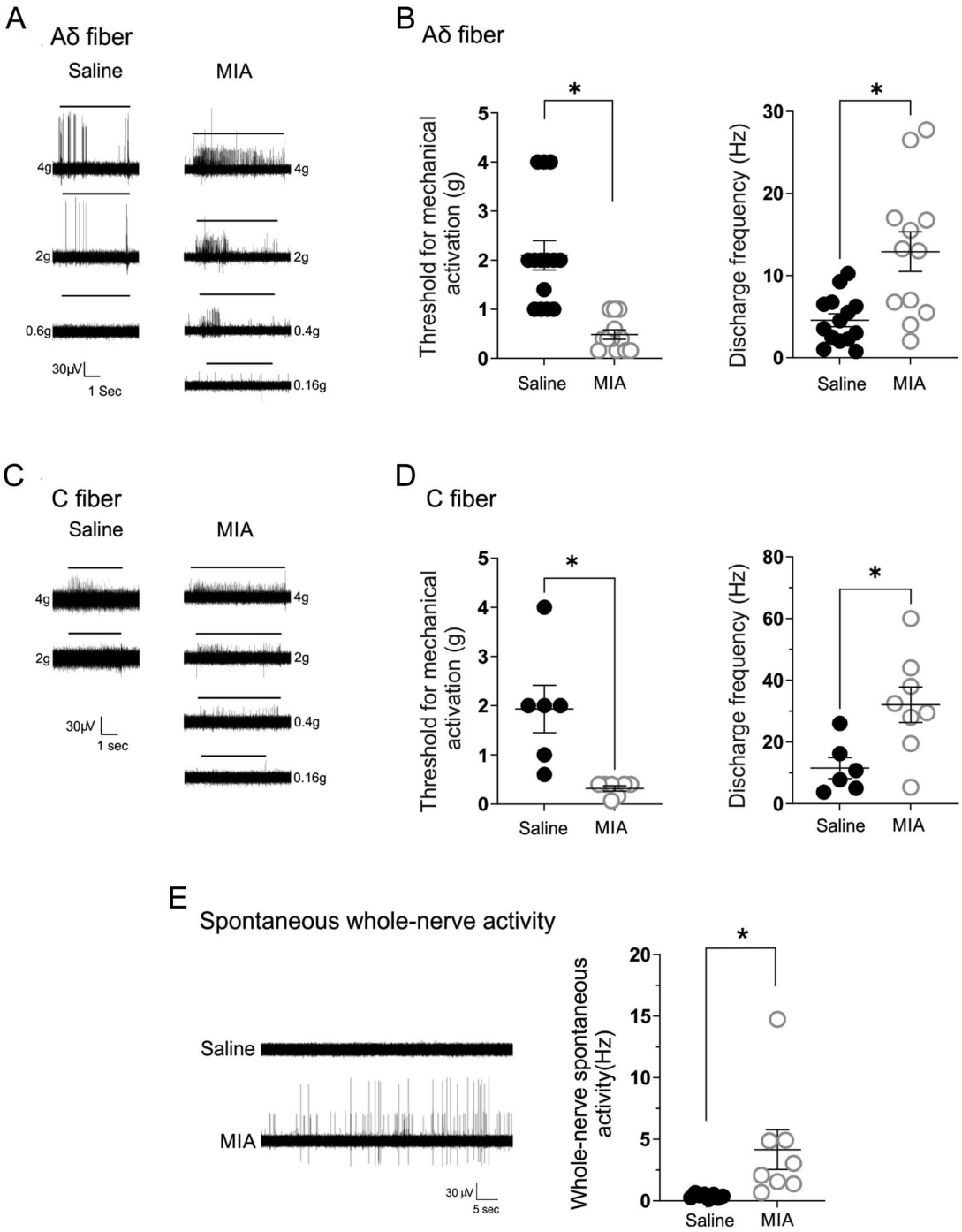

Figure 4. Monoiodoacetate-induced changes to function of knee joint afferent neurons at day. (A) Raw traces showing the response of Aδ knee joint afferent neurons to von Frey stimulation at various forces. Left column shows a neuron recorded 3 days after saline injection. Right column shows a neuron recorded 3 days after MIA injection. (B) Group data showing a decrease in threshold for activation (left; nested *t* test, $^*P < 0.05$) and an increase in discharge frequency (right; nested *t* test, $^*P < 0.05$) for single Aδ knee joint afferent neurons recorded at day 3 post-MIA (N = 12, n = 8), relative to saline (N = 14, n = 8) injection. (C) Raw traces showing the response of C knee joint afferent neurons to von Frey stimulation at various forces. Left column shows a neuron recorded 3 days after saline injection. Right column shows a neuron recorded 3 days after MIA injection. D, Group data showing a decrease in threshold for activation (left; nested *t* test, $^*P < 0.05$) and an increase in discharge frequency (right; nested *t* test, $^*P < 0.05$) for single C knee joint afferent neurons recorded at day 3 post-MIA (N = 8, n = 7), relative to saline (N = 6, n = 6) injection. E, Raw traces (left) and group data (right; unpaired *t* test, $^*P < 0.05$) showing a change in spontaneous activity of knee joint nerves recorded 3 days after MIA (n = 8), relative to saline (n = 8) injection. Data represent mean ± SEM. MIA, monoiodoacetate.

a role for changes in the function of nerves innervating the surrounding tissues such as bone at this early stage. Interestingly, our findings indicate that although some (C-fiber) knee joint afferent neurons continue to be sensitized in late-MIA-induced OA, there is a distinct lack of spontaneous activity in the medial articular nerve, and some (Aδ-fiber) knee joint afferent neurons do not have altered activity levels at this late time-point. Furthermore, this seems to be associated with less defined histological changes in the synovium and joint capsule in late, relative to early, MIA-induced OA. Thus, knee joint afferent neurons may be particularly important during acute inflammation of the knee and may have less of a contribution to pain signaling in late MIA-

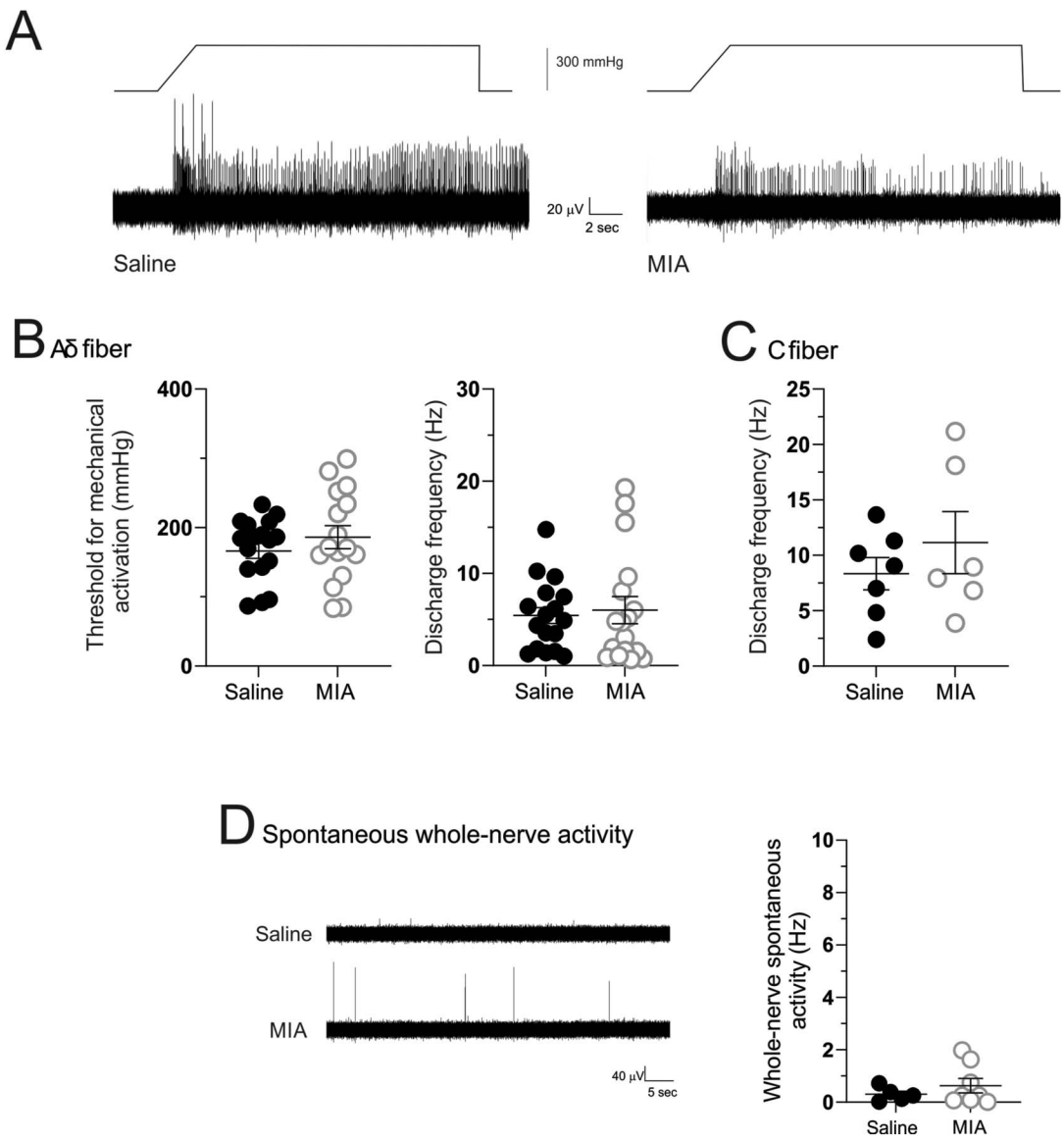

Figure 5. Monoiodoacetate-induced changes to function of bone afferent neurons at day 3. (A) Raw traces showing the response of bone afferent neurons, in whole-nerve recordings, to a ramp-and-hold intraosseous pressure stimulus 3 days after saline (left) or MIA (right) injections into the knee joint. (B) Group data showing no change in threshold for activation (left; nested *t* test), or in discharge frequency (right; nested *t* test), for single Aδ bone afferent neurons recorded at day 3 post-MIA (N = 17, n = 7), relative to saline (N = 17, n = 7) injection. (C) Group data showing no change in discharge frequency (unpaired *t* test) for all C bone afferent neurons in whole-nerve recordings, at day 3 post-MIA (n = 6), relative to saline (n = 7) injection. (D) Raw traces (left) and group data (right; unpaired *t* test) showing no change in spontaneous activity of the bone nerve recorded 3 days after MIA (n = 8) relative to saline (n = 5) injection. Data represent mean ± SEM. MIA, monoiodoacetate.

induced OA when there is less evidence of inflammation in the joint.

Severe pain in late OA is the main reason that patients present to the clinical environment, and it predisposes patients to knee joint replacement therapy.[32,52,64] Thus, understanding the pathogenesis of pain at this late stage of disease is critical for the development of targeted therapies to treat it. Although synovitis presents in late-stage OA, and there is a documented association between synovitis and pain, the severity of the damage to the joint capsule and synovium bears little relation to the severity of the pain experienced.[9,17,34,38] This suggests that activation and/or sensitization of articular nociceptors may not be the only drivers of severe pain experienced by patients with OA. By contrast, severe pain in patients with late OA is clearly correlated with radiological evidence of subchondral bone lesions and/or inflammation, and the severity of the pain is correlated with the size of the lesions.[1,13,16,36,60,75] For example, Felson et al.[16] performed a cross-sectional observational study on 401 patients with knee OA using visual analogue and WOMAC scales to capture pain outcomes. They reported that subchondral bone lesions were found in 272 of 351 (77.5%) patients with painful knees vs 15 of 50 (30%) patients without knee pain, and that the size of the bone lesion was independently associated with pain. Aso et al.[1] more recently reported, in another cross-sectional study on over 1400 patients, that the size of bone marrow lesions correlated specifically with weight-bearing pain.

Our finding that changes in the function of bone afferent neurons only occur late in MIA-induced OA, when there is histological evidence of damage to the articular cartilage and surrounding subchondral bone, further suggests that the

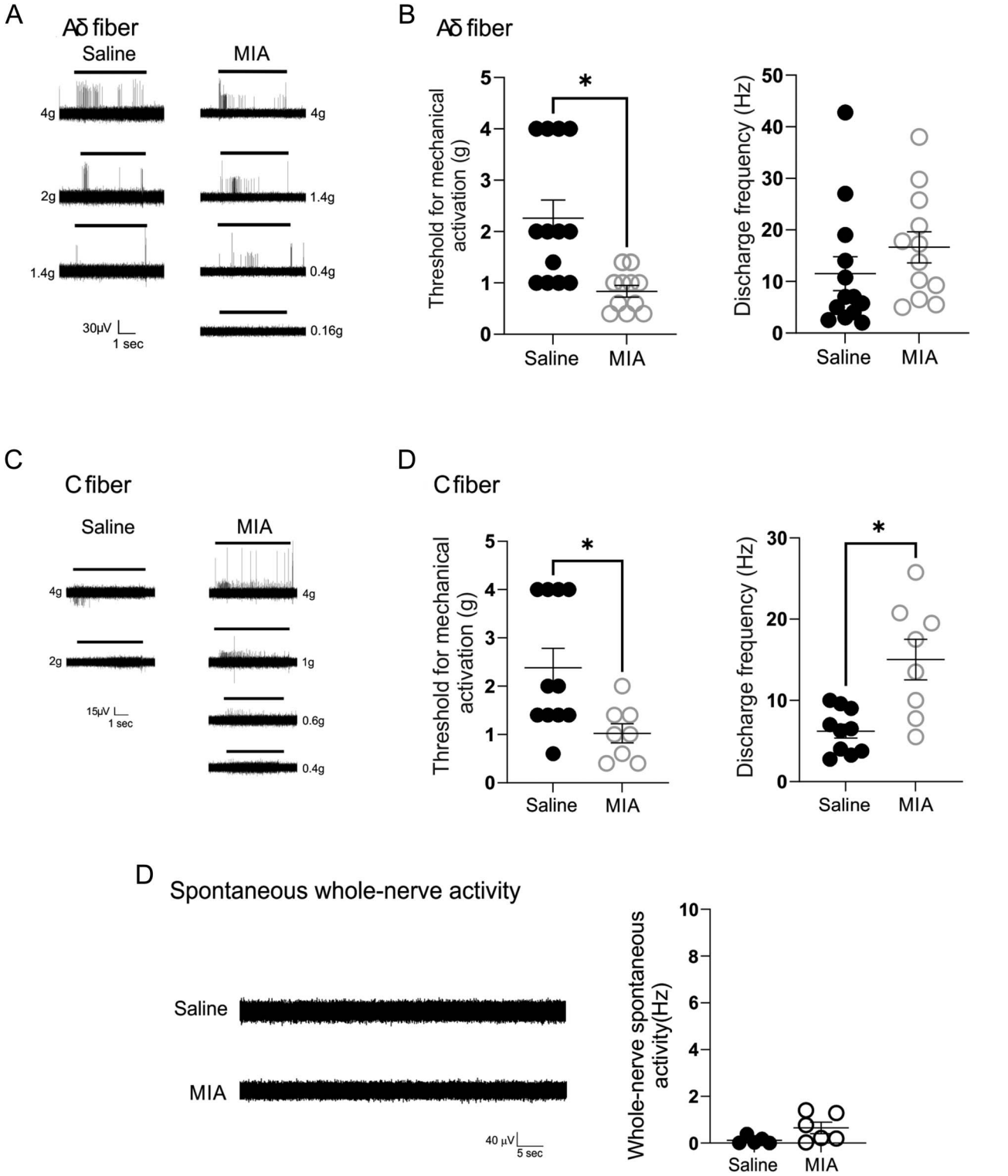

Figure 6. Monoiodoacetate-induced changes to function of knee joint afferent neurons at day 28. (A) Raw traces showing the response of Aδ knee joint afferent neurons to von Frey stimulation at various forces. Left column shows a neuron recorded 28 days after saline injection. Right column shows a neuron recorded 28 days after MIA injection. (B) Group data showing a decrease in threshold for activation (left; nested *t* test, $^*P < 0.05$), but no change in discharge frequency (right; nested *t* test), for single Aδ knee joint afferent neurons recorded at day 28 post-MIA (N = 12, n = 8), relative to saline (N = 13, n = 9) injection. (C) Raw traces showing the response of C knee joint afferent neurons to von Frey stimulation at various forces. Left column shows a neuron recorded 28 days after saline injection. Right column shows a neuron recorded 28 days after MIA injection. (D) Group data showing a decrease in threshold for activation (left; nested *t* test, $^*P < 0.05$) and an increase in discharge frequency (right; nested *t* test, $^*P < 0.05$) for single C knee joint afferent neurons recorded at day 28 post-MIA (N = 8, n = 5), relative to saline (N = 11, n = 7) injection. (E) Raw traces (left) and group data (right; unpaired *t* test) showing no change in spontaneous activity of whole nerves recorded 28 days after MIA (n = 6) relative to saline (n = 5) injection. Data represent mean ± S.E.M. MIA, monoiodoacetate.

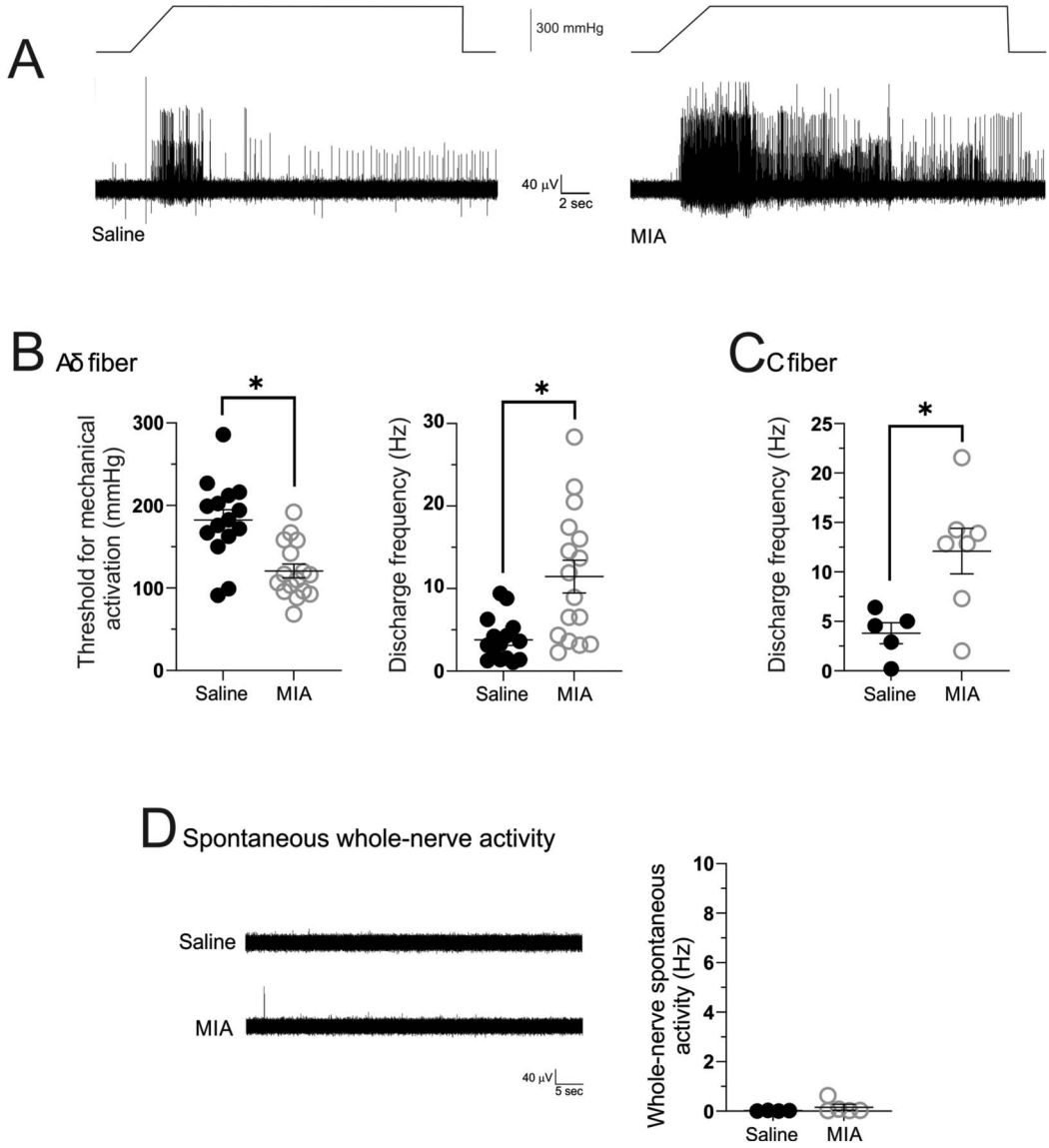

Figure 7. Monoiodoacetate-induced changes to function of bone afferent neurons at day 28. (A) Raw traces showing the response of bone afferent neurons, in whole-nerve recordings, to a ramp-and-hold intraosseous pressure stimulus 28 days after saline (left) or MIA (right) injections into the knee joint. (B) Group data showing a decrease in threshold for activation (left; nested *t* test, $^*P < 0.05$) and an increase in discharge frequency (right; nested *t* test, $^*P < 0.05$) for single Aδ bone afferent neurons recorded at day 28 post-MIA (N = 16, n = 6), relative to saline (N = 15, n = 6) injection. (C) Group data showing an increase in discharge frequency (unpaired *t* test, $^*P < 0.05$) for all C bone afferent neurons in whole-nerve recordings, at day 28 post-MIA (n = 7) relative to saline (n = 5) injection. (D) Raw traces (left) and group data (right; unpaired *t* test) showing no change in spontaneous activity of the bone nerve recorded 28 days after MIA (n = 5) relative to saline (n = 4) injection. Data represent mean ± SEM. MIA, monoiodoacetate.

severe pain late in disease progression involves nerves that innervate the subchondral bone. A number of recent studies have reported that bone afferent neurons can be activated and sensitized by inflammatory mediators in bone, and/or respond to noxious mechanical stimulation,[44,45,47–50] providing mechanisms by which their function could be modulated in OA. There is also evidence of changes to the sensory innervation of subchondral bone in humans with OA,[56,71] and in a number of murine models of OA, including OA induced by mechanical joint loading,[73] anterior cruciate ligament tear,[78] destabilization of the medial meniscus,[53] or in the lumbar facet joint.[35] These findings are important because they highlight the need to target the peripheral sensory neurons that innervate bone, in addition to those that innervate the joint, for therapeutic benefit in late-stage OA to be realized.

There is also emerging evidence for a role for neuropathy of peripheral sensory neurons in the pathophysiology of OA.[20,40,41] It is possible that the physiological changes to the function of bone afferent neurons we have reported here are a response to damage of their peripheral nerve terminal endings in subchondral bone, resulting from destruction and/or remodeling of bone in late-stage OA. It will be important in the future to determine whether neuropathy affects bone afferent neurons and their contribution to the pathogenesis of OA.

Identifying mechanisms related to the different stages of OA is important because it could direct specific pain therapies to different stages of the disease. In rat MIA-induced OA, NSAIDs reverse weight-bearing pain and hyperalgesia in the first 2 weeks after induction, but in later stages, only centrally acting drugs such as morphine and gabapentin are effective.[3,19,55] One of these studies

confirmed that naproxen, an NSAID, also blocked spontaneous activity from joint afferent neurons only during the early phase.[19] Bisphosphonates also reduce pain behavior in MIA-induced OA,[77] and it seems they may reverse OA-induced pain when there is clear evidence of alterations to subchondral bone innervation.[78] They might be most beneficial in certain subsets of patients with OA who display high rates of subchondral bone turnover.[76] Thus, it may be necessary for novel therapies designed to treat OA pain to target neuronal populations that innervate different tissues, and at different stages of disease. Our new finding that pain in late MIA-induced OA is associated with changes to the function of nerves that innervate subchondral bone suggests that they are likely to be important targets for development of mechanism-based therapies to treat pain late in disease progression.

Conflict of interest statement

The authors have no conflicts of interest to declare.

Acknowledgements

This work was supported by funding from the National Health and Medical Research Council NHMRC #1185981.

Supplemental video content

A video abstract associated with this article can be found at http://links.lww.com/PAIN/B400.

Article history:
Received 30 March 2021
Received in revised form 20 April 2021
Accepted 7 May 2021
Available online 3 June 2021

References

[1] Aso K, Shahtaheri SM, McWilliams DF, Walsh DA. Association of subchondral bone marrow lesion localization with weight-bearing pain in people with knee osteoarthritis: data from the Osteoarthritis Initiative. Arthritis Res Ther 2021;23:35.
[2] Berenbaum F. Osteoarthritis as an inflammatory disease (osteoarthritis is not osteoarthrosis!). Osteoarthritis Cartilage 2013;21:16.
[3] Bove SE, Calcaterra SL, Brooker RM, Huber CM, Guzman RE, Juneau PL, Schrier DJ, Kilgore KS. Weight bearing as a measure of disease progression and efficacy of anti-inflammatory compounds in a model of monosodium iodoacetate-induced osteoarthritis. Osteoarthritis Cartilage 2003;11:821–30.
[4] Brederson JD, Chu KL, Xu J, Nikkel AL, Markosyan S, Jarvis MF, Edelmayer R, Bitner RS, McGaraughty S. Characterization and comparison of rat monosodium iodoacetate and medial meniscal tear models of osteoarthritic pain. J Orthop Res 2018;36:2109–17.
[5] Brenn D, Richter F, Schaible HG. Sensitization of unmyelinated sensory fibers of the joint nerve to mechanical stimuli by interleukin-6 in the rat: an inflammatory mechanism of joint pain. Arthritis Rheum 2007;56:351–9.
[6] Brucini M, Duranti R, Galletti R, Pantaleo T, Zucchi PL. Pain thresholds and electromyographic features of periarticular muscles in patients with osteoarthritis of the knee. PAIN 1981;10:57–66.
[7] Burr DB, Radin EL. Microfractures and microcracks in subchondral bone: are they relevant to osteoarthrosis?. Rheum Dis Clin North Am 2003;29:675–85.
[8] Chu KL, Chandran P, Joshi SK, Jarvis MF, Kym PR, McGaraughty S. TRPV1-related modulation of spinal neuronal activity and behavior in a rat model of osteoarthritic pain. Brain Res 2011;1369:158–66.
[9] Davis MA, Ettinger WH, Neuhaus JM, Barclay JD, Segal MR. Correlates of knee pain among US adults with and without radiographic knee osteoarthritis. J Rheumatol 1992;19:1943–9.
[10] Dieppe P. Subchondral bone should be the main target for the treatment of pain and disease progression in osteoarthritis. Osteoarthritis Cartilage 1999;7:325–6.
[11] Dieppe PA, Lohmander LS. Pathogenesis and management of pain in osteoarthritis. Lancet 2005;365:965–73.
[12] Dorn T, Schaible HG, Schmidt RF. Response properties of thick myelinated group II afferents in the medial articular nerve of normal and inflamed knee joints of the cat. Somatosens Mot Res 1991;8:127–36.
[13] Driban JB, Price L, Lo GH, Pang J, Hunter DJ, Miller E, Ward RJ, Eaton CB, Lynch JA, McAlindon TE. Evaluation of bone marrow lesion volume as a knee osteoarthritis biomarker–longitudinal relationships with pain and structural changes: data from the Osteoarthritis Initiative. Arthritis Res Ther 2013;15:R112.
[14] Emery CA, Whittaker JL, Mahmoudian A, Lohmander LS, Roos EM, Bennell KL, Toomey CM, Reimer RA, Thompson D, Ronsky JL, Kuntze G, Lloyd DG, Andriacchi T, Englund M, Kraus VB, Losina E, Bierma-Zeinstra S, Runhaar J, Peat G, Luyten FP, Snyder-Mackler L, Risberg MA, Mobasheri A, Guermazi A, Hunter DJ, Arden NK. Establishing outcome measures in early knee osteoarthritis. Nat Rev Rheumatol 2019;15:438–48.
[15] Felson DT. Developments in the clinical understanding of osteoarthritis. Arthritis Res Ther 2009;11:203.
[16] Felson DT, Chaisson CE, Hill CL, Totterman SM, Gale ME, Skinner KM, Kazis L, Gale DR. The association of bone marrow lesions with pain in knee osteoarthritis. Ann Intern Med 2001;134:541–9.
[17] Felson DT, Lawrence RC, Dieppe PA, Hirsch R, Helmick CG, Jordan JM, Kington RS, Lane NE, Nevitt MC, Zhang Y, Sowers M, McAlindon T, Spector TD, Poole AR, Yanovski SZ, Ateshian G, Sharma L, Buckwalter JA, Brandt KD, Fries JF. Osteoarthritis: new insights. Part 1: the disease and its risk factors. Ann Intern Med 2000;133:635–46.
[18] Felson DT, McLaughlin S, Goggins J, LaValley MP, Gale ME, Totterman S, Li W, Hill C, Gale D. Bone marrow edema and its relation to progression of knee osteoarthritis. Ann Intern Med 2003;139:330–6.
[19] Fernihough J, Gentry C, Malcangio M, Fox A, Rediske J, Pellas T, Kidd B, Bevan S, Winter J. Pain related behaviour in two models of osteoarthritis in the rat knee. PAIN 2004;112:83–93.
[20] Fu K, Robbins SR, McDougall JJ. Osteoarthritis: the genesis of pain. Rheumatology (Oxford) 2018;57:iv43–iv50.
[21] Gerwin N, Bendele AM, Glasson S, Carlson CS. The OARSI histopathology initiative - recommendations for histological assessments of osteoarthritis in the rat. Osteoarthritis Cartilage 2010;18:S24–34.
[22] Grigg P, Schaible HG, Schmidt RF. Mechanical sensitivity of group III and IV afferents from posterior articular nerve in normal and inflamed cat knee. J Neurophysiol 1986;55:635–43.
[23] Grubb BD. Activation of sensory neurons in the arthritic joint. Novartis Found Symp 2004;260:28–36; discussion 36-48, 100-104, 277-109.
[24] Hatch RJ, Jennings EA, Ivanusic JJ. Peripheral hyperpolarization-activated cyclic nucleotide-gated channels contribute to inflammation-induced hypersensitivity of the rat temporomandibular joint. Eur J Pain 2013;17:972–82.
[25] Hensor EM, Dube B, Kingsbury SR, Tennant A, Conaghan PG. Toward a clinical definition of early osteoarthritis: onset of patient-reported knee pain begins on stairs. Data from the osteoarthritis initiative. Arthritis Care Res (Hoboken) 2015;67:40–7.
[26] Hill CL, Hunter DJ, Niu J, Clancy M, Guermazi A, Genant H, Gale D, Grainger A, Conaghan P, Felson DT. Synovitis detected on magnetic resonance imaging and its relation to pain and cartilage loss in knee osteoarthritis. Ann Rheum Dis 2007;66:1599–603.
[27] Ivanusic JJ. Molecular mechanisms that contribute to bone marrow pain. Front Neurol 2017;8:458.
[28] Ivanusic JJ, Beaini D, Hatch RJ, Staikopoulos V, Sessle BJ, Jennings EA. Peripheral N-methyl-d-aspartate receptors contribute to mechanical hypersensitivity in a rat model of inflammatory temporomandibular joint pain. Eur J Pain 2011;15:179–85.
[29] Just S, Pawlak M, Heppelmann B. Responses of fine primary afferent nerve fibres innervating the rat knee joint to defined torque. J Neurosci Methods 2000;103:157–62.
[30] Kellgren JH, Lawrence JS. Radiological assessment of osteo-arthrosis. Ann Rheum Dis 1957;16:494–502.
[31] Kidd BL, Photiou A, Inglis JJ. The role of inflammatory mediators on nociception and pain in arthritis. Novartis Found Symp 2004;260:122–33.
[32] Klement MR, Sharkey PF. The significance of osteoarthritis-associated bone marrow lesions in the knee. J Am Acad Orthop Surg 2019;27:752–9.
[33] Krustev E, Rioux D, McDougall JJ. Mechanisms and mediators that drive arthritis pain. Curr Osteoporos Rep 2015;13:216–24.
[34] Lawrence JS, Bremner JM, Bier F. Osteo-arthrosis. Prevalence in the population and relationship between symptoms and x-ray changes. Ann Rheum Dis 1966;25:1–24.

[35] Li J, Ding Z, Li Y, Wang W, Wang J, Yu H, Liu A, Miao J, Chen S, Wu T, Cao Y. BMSCs-derived exosomes ameliorate pain via abrogation of aberrant nerve invasion in subchondral bone in lumbar facet joint osteoarthritis. J Orthop Res 2020;38:670–9.
[36] Link TM, Steinbach LS, Ghosh S, Ries M, Lu Y, Lane N, Majumdar S. Osteoarthritis: MR imaging findings in different stages of disease and correlation with clinical findings. Radiology 2003;226:373–81.
[37] Luyten FP, Bierma-Zeinstra S, Dell'Accio F, Kraus VB, Nakata K, Sekiya I, Arden NK, Lohmander LS. Toward classification criteria for early osteoarthritis of the knee. Semin Arthritis Rheum 2018;47:457–63.
[38] McAlindon TE, Cooper C, Kirwan JR, Dieppe PA. Knee pain and disability in the community. Br J Rheumatol 1992;31:189–92.
[39] McDougall JJ. Arthritis and pain. Neurogenic origin of joint pain. Arthritis Res Ther 2006;8:220.
[40] McDougall JJ, Albacete S, Schuelert N, Mitchell PG, Lin C, Oskins JL, Bui HH, Chambers MG. Lysophosphatidic acid provides a missing link between osteoarthritis and joint neuropathic pain. Osteoarthritis Cartilage 2017;25:926–34.
[41] McDougall JJ, Linton P. Neurophysiology of arthritis pain. Curr Pain Headache Rep 2012;16:485–91.
[42] Miller RE, Malfait AM. Osteoarthritis pain: what are we learning from animal models? Best Pract Res Clin Rheumatol 2017;31:676–87.
[43] Miranda JA, Stanley P, Gore K, Turner J, Dias R, Rees H. A preclinical physiological assay to test modulation of knee joint pain in the spinal cord: effects of oxycodone and naproxen. PLoS One 2014;9:e106108.
[44] Morgan M, Nencini S, Thai J, Ivanusic JJ. TRPV1 activation alters the function of Adelta and C fiber sensory neurons that innervate bone. Bone 2019;123:168–75.
[45] Morgan M, Thai J, Trinh P, Habib M, Effendi KN, Ivanusic JJ. ASIC3 inhibition modulates inflammation-induced changes in the activity and sensitivity of Adelta and C fiber sensory neurons that innervate bone. Mol Pain 2020;16:1744806920975950.
[46] Mousseau M, Burma NE, Lee KY, Leduc-Pessah H, Kwok CHT, Reid AR, O'Brien M, Sagalajev B, Stratton JA, Patrick N, Stemkowski PL, Biernaskie J, Zamponi GW, Salo P, McDougall JJ, Prescott SA, Matyas JR, Trang T. Microglial pannexin-1 channel activation is a spinal determinant of joint pain. Sci Adv 2018;4:eaas9846.
[47] Nencini S, Ivanusic J. Mechanically sensitive Adelta nociceptors that innervate bone marrow respond to changes in intra-osseous pressure. J Physiol 2017;595:4399–415.
[48] Nencini S, Ringuet M, Kim DH, Chen YJ, Greenhill C, Ivanusic JJ. Mechanisms of nerve growth factor signaling in bone nociceptors and in an animal model of inflammatory bone pain. Mol Pain 2017;13:1744806917697011.
[49] Nencini S, Ringuet M, Kim DH, Greenhill C, Ivanusic JJ. GDNF, neurturin, and artemin activate and sensitize bone afferent neurons and contribute to inflammatory bone pain. J Neurosci 2018;38:4899–911.
[50] Nencini S, Thai J, Ivanusic JJ. Sequestration of artemin reduces inflammation-induced activation and sensitization of bone marrow nociceptors in a rodent model of carrageenan-induced inflammatory bone pain. Eur J Pain 2019;23:397–409.
[51] Neugebauer V, Schaible HG, Schmidt RF. Sensitization of articular afferents to mechanical stimuli by bradykinin. Pflugers Arch 1989;415:330–5.
[52] Nielsen FK, Egund N, Jorgensen A, Jurik AG. Risk factors for joint replacement in knee osteoarthritis; a 15-year follow-up study. BMC Musculoskelet Disord 2017;18:510.
[53] Obeidat AM, Miller RE, Miller RJ, Malfait AM. The nociceptive innervation of the normal and osteoarthritic mouse knee. Osteoarthritis Cartilage 2019;27:1669–79.
[54] Philpott HT, O'Brien M, McDougall JJ. Attenuation of early phase inflammation by cannabidiol prevents pain and nerve damage in rat osteoarthritis. PAIN 2017;158:2442–51.
[55] Rashid MH, Theberge Y, Elmes SJ, Perkins MN, McIntosh F. Pharmacological validation of early and late phase of rat mono-iodoacetate model using the Tekscan system. Eur J Pain 2013;17:210–22.
[56] Reimann I, Christensen SB. A histological demonstration of nerves in subchondral bone. Acta Orthop Scand 1977;48:345–52.
[57] Richter F, Natura G, Ebbinghaus M, von Banchet GS, Hensellek S, Konig C, Brauer R, Schaible HG. Interleukin-17 sensitizes joint nociceptors to mechanical stimuli and contributes to arthritic pain through neuronal interleukin-17 receptors in rodents. Arthritis Rheum 2012;64:4125–34.
[58] Richter F, Natura G, Loser S, Schmidt K, Viisanen H, Schaible HG. Tumor necrosis factor causes persistent sensitization of joint nociceptors to mechanical stimuli in rats. Arthritis Rheum 2010;62:3806–14.
[59] Sagar DR, Nwosu L, Walsh DA, Chapman V. Dissecting the contribution of knee joint NGF to spinal nociceptive sensitization in a model of OA pain in the rat. Osteoarthritis Cartilage 2015;23:906–13.
[60] Sansone V, Maiorano E, Pascale V, Romeo P. Bone marrow lesions of the knee: longitudinal correlation between lesion size changes and pain before and after conservative treatment by extracorporeal shockwave therapy. Eur J Phys Rehabil Med 2019;55:225–30.
[61] Schaible HG, Schmidt RF. Effects of an experimental arthritis on the sensory properties of fine articular afferent units. J Neurophysiol 1985;54:1109–22.
[62] Schaible HG, Schmidt RF. Discharge characteristics of receptors with fine afferents from normal and inflamed joints: influence of analgesics and prostaglandins. Agents Actions Suppl 1986;19:99–117.
[63] Schepelmann K, Messlinger K, Schaible HG, Schmidt RF. Inflammatory mediators and nociception in the joint: excitation and sensitization of slowly conducting afferent fibers of cat's knee by prostaglandin I2. Neuroscience 1992;50:237–47.
[64] Scher C, Craig J, Nelson F. Bone marrow edema in the knee in osteoarthrosis and association with total knee arthroplasty within a three-year follow-up. Skeletal Radiol 2008;37:609–17.
[65] Schuelert N, McDougall JJ. Electrophysiological evidence that the vasoactive intestinal peptide receptor antagonist VIP6-28 reduces nociception in an animal model of osteoarthritis. Osteoarthritis Cartilage 2006;14:1155–62.
[66] Schuelert N, McDougall JJ. Cannabinoid-mediated antinociception is enhanced in rat osteoarthritic knees. Arthritis Rheum 2008;58:145–53.
[67] Schuelert N, McDougall JJ. Grading of monosodium iodoacetate-induced osteoarthritis reveals a concentration-dependent sensitization of nociceptors in the knee joint of the rat. Neurosci Lett 2009;465:184–8.
[68] Schuelert N, McDougall JJ. Involvement of Nav 1.8 sodium ion channels in the transduction of mechanical pain in a rodent model of osteoarthritis. Arthritis Res Ther 2012;14:R5.
[69] Schuelert N, Zhang C, Mogg AJ, Broad LM, Hepburn DL, Nisenbaum ES, Johnson MP, McDougall JJ. Paradoxical effects of the cannabinoid CB2 receptor agonist GW405833 on rat osteoarthritic knee joint pain. Osteoarthritis Cartilage 2010;18:1536–43.
[70] Simkin PA. Bone pain and pressure in osteoarthritic joints. Novartis Found Symp 2004;260:179–86; discussion 186-190, 277-179.
[71] Suri S, Gill SE, Massena de Camin S, Wilson D, McWilliams DF, Walsh DA. Neurovascular invasion at the osteochondral junction and in osteophytes in osteoarthritis. Ann Rheum Dis 2007;66:1423–8.
[72] Suri S, Walsh DA. Osteochondral alterations in osteoarthritis. Bone 2012;51:204–11.
[73] Ter Heegde F, Luiz AP, Santana-Varela S, Magnusdottir R, Hopkinson M, Chang Y, Poulet B, Fowkes RC, Wood JN, Chenu C. Osteoarthritis-related nociceptive behaviour following mechanical joint loading correlates with cartilage damage. Osteoarthritis Cartilage 2020;28:383–95.
[74] Thai J, Kyloh M, Travis L, Spencer NJ, Ivanusic JJ. Identifying spinal afferent (sensory) nerve endings that innervate the marrow cavity and periosteum using anterograde tracing. J Comp Neurol 2020;528:1903–16.
[75] Torres L, Dunlop DD, Peterfy C, Guermazi A, Prasad P, Hayes KW, Song J, Cahue S, Chang A, Marshall M, Sharma L. The relationship between specific tissue lesions and pain severity in persons with knee osteoarthritis. Osteoarthritis Cartilage 2006;14:1033–40.
[76] Vaysbrot EE, Osani MC, Musetti MC, McAlindon TE, Bannuru RR. Are bisphosphonates efficacious in knee osteoarthritis? A meta-analysis of randomized controlled trials. Osteoarthritis Cartilage 2018;26:154–64.
[77] Yu D, Liu F, Liu M, Zhao X, Wang X, Li Y, Mao Y, Zhu Z. The inhibition of subchondral bone lesions significantly reversed the weight-bearing deficit and the overexpression of CGRP in DRG neurons, GFAP and Iba-1 in the spinal dorsal horn in the monosodium iodoacetate induced model of osteoarthritis pain. PLoS One 2013;8:e77824.
[78] Zhu S, Zhu J, Zhen G, Hu Y, An S, Li Y, Zheng Q, Chen Z, Yang Y, Wan M, Skolasky RL, Cao Y, Wu T, Gao B, Yang M, Gao M, Kuliwaba J, Ni S, Wang L, Wu C, Findlay D, Eltzschig HK, Ouyang HW, Crane J, Zhou FQ, Guan Y, Dong X, Cao X. Subchondral bone osteoclasts induce sensory innervation and osteoarthritis pain. J Clin Invest 2019;129:1076–93.